J. Fluid Mech. (2008), *vol.* 614, *pp.* 447–470.
doi:10.1017/S0022112008003509 Printed in the United Kingdom

On the entrainment coefficient in negatively buoyant jets

PANOS N. PAPANICOLAOU[1], ILIAS G. PAPAKONSTANTIS[2] AND GEORGE C. CHRISTODOULOU[2]

[1]Department of Civil Engineering, University of Thessaly, Pedion Areos, 38334 Volos, Greece
panospap@uth.gr

[2]School of Civil Engineering, National Technical University of Athens, 5 Heroon Polytechniou Street, 15780 Zografou, Athens, Greece

(Received 28 September 2007 and in revised form 10 July 2008)

Integral models proposed to simulate positively buoyant jets are used to model jets with negative or reversing buoyancy issuing into a calm, homogeneous or density-stratified environment. On the basis of the self-similarity assumption, 'top hat' and Gaussian cross-sectional distributions are employed for concentration and velocity. The entrainment coefficient is considered to vary with the local Richardson number, between the asymptotic values for simple jets and plumes, estimated from earlier experiments in positively buoyant jets. Top-hat and Gaussian distribution models are employed in a wide range of experimental data on negatively buoyant jets, issuing vertically or at an angle into a calm homogeneous ambient, and on jets with reversing buoyancy, discharging into a calm, density-stratified fluid. It is found that geometrical characteristics such as the terminal (steady state) height of rise, the spreading elevation in stratified ambient and the distance to the point of impingement are considerably underestimated, resulting in lower dilution rates at the point of impingement, especially when the Gaussian formulation is applied. Reduction of the entrainment coefficient in the jet-like flow regime improves model predictions, indicating that the negative buoyancy reduces the entrainment in momentum-driven, negatively buoyant jets.

1. Introduction

Liquid wastes from desalination or geothermal plants, as well as from industrial operations, are usually heavier than the receiving ambient waters. Frequently, these liquids are discharged into a water body as negatively buoyant jets. Also, an initially positively buoyant jet in a density-stratified ambient will eventually become negatively buoyant, once it passes through the elevation of neutral buoyancy (mean spreading elevation). The environmental impact of negatively buoyant jet discharges can be predicted once we evaluate the basic properties of a dense jet, such as spreading distances and dilution. This is usually obtained via physical or computational modelling.

Several (mainly one-dimensional) computational models regarding steady state buoyant jets have been proposed in the past. Recently, Wang & Law (2002) and Yannopoulos (2006) have proposed second-order integral models for vertical, positively buoyant jets, which take into consideration the turbulent mass and momentum fluxes. Jirka (2004) has proposed an integral model widely known as

Corjet to simulate buoyant jets discharging at different angles with respect to the horizontal in an unbound ambient fluid with uniform density or stable density stratification under stagnant or steady sheared current conditions. This model has been compared with experimental data of earlier investigations, with a very good overall agreement when applied to positively buoyant jets.

The entrainment hypothesis relating the inflow velocity to the mean local one in turbulent shear flows is summarized by Turner (1986), who has discussed in detail the turbulent entrainment rate in several types of such flows. The entrainment coefficient α in positively buoyant jets is generally assumed to be variable. Experiments suggest that α takes the asymptotic values α_j and α_p in momentum-driven (jet-like) and buoyancy-driven (plume-like) flows respectively and the values in between at the transition from jets to plumes. The evaluation of the entrainment coefficient, used in integral models, has been studied in the past. It is usually obtained through expressions of its asymptotic values and the local buoyant jet Richardson number $R(s)$, s being the distance from the origin along the jet axis. An expression proposed by Priestley & Ball (1955) is based on the conservation of energy and reads

$$\alpha = \alpha_j - (\alpha_j - \alpha_p)\left(\frac{R(s)}{R_p}\right)^2, \tag{1}$$

where R_p is the limiting, plume Richardson number. A second empirical formula proposed by List (1982) is

$$\alpha = \alpha_j \exp\left[\ln\left(\frac{\alpha_p}{\alpha_j}\right)\left(\frac{R(s)}{R_p}\right)^2\right]. \tag{2}$$

The local Richardson number $R(s)$ in a buoyant jet is defined as

$$R(s) = \frac{\mu(s)\beta(s)^{1/2}}{m(s)^{5/4}}, \tag{3}$$

where $\mu(s)$, $m(s)$ and $\beta(s)$ respectively are the specific mass, momentum and buoyancy fluxes at a distance s from the origin. Typical values for these parameters have been estimated by Fischer *et al.* (1979) and List (1982) to be $\alpha_j = 0.0535$, $\alpha_p = 0.0833$ and $R_p = 0.557$. They have also been evaluated experimentally by Papanicolaou & List (1988), who suggested the values $\alpha_j = 0.0545$, $\alpha_p = 0.0875$ and $R_p = 0.63$, where R_p was computed using the momentum flux due to the mean flow. More recently, Jirka (2004) has employed an expression similar to that proposed by Priestley & Ball (1955) for the entrainment coefficient, introducing the local densimetric Froude number instead of the Richardson number, yielding the values $\alpha_j = 0.055$, $\alpha_p = 0.083$ and $R_p = 0.522$ (computed from the corresponding Froude number 4.67).

Negatively buoyant jets have been investigated in experimental studies by several researchers. Experiments regarding the maximum (initial) and terminal (steady state) penetration heights in vertical negatively buoyant round jets (figure 1*a*) have been reported by Turner (1966), Baines, Turner & Campbell (1990), Lindberg (1994), Zhang & Baddour (1998) and Bloomfield & Kerr (2000) and recently by Papanicolaou & Kokkalis (2008). Experiments on inclined dense jets (figure 1*b*) regarding geometrical characteristics such as the rise height and the distance from the point of impingement have been reported by Zeitoun, McIlhenny & Reid (1970), Roberts & Toms (1987), Roberts, Ferrier & Daviero (1997), Lindberg (1994) and Bloomfield & Kerr (2002) and recently by Papakonstantis, Kampourelli & Christodoulou (2007). However, only Roberts & Toms (1987) and Roberts *et al.* (1997) have provided results about dilution.

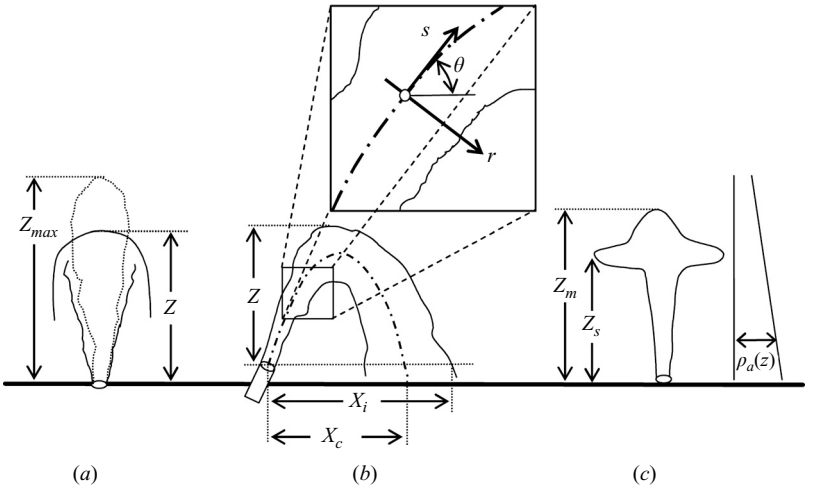

FIGURE 1. Definition diagram for (*a*) vertical negatively buoyant jet in uniform ambient, (*b*) inclined negatively buoyant jet in uniform ambient and (*c*) vertical buoyant jet in linearly density-stratified ambient.

Vertical round buoyant jets in a linearly density-stratified calm ambient (figure 1*c*), have been reported by Fan (1967), Wong & Wright (1988), Bloomfield & Kerr (1998) and Konstantinidou & Papanicolaou (2003). The data from these experiments could potentially be used to evaluate numerical models, which may be employed for prediction.

Wong & Wright (1988) used a Gaussian model to predict the maximum height of rise of round, vertical buoyant jets in a linearly stratified calm ambient. In the regime of initially jet-like flows, the maximum rise height was substantially underestimated if compared to that obtained experimentally. Konstantinidou & Papanicolaou (2003) proposed a reduced value of the jet entrainment coefficient in order to match the measured maximum height of rise of vertical jets in linearly density-stratified fluid with that estimated by Gaussian one-dimensional modelling.

Papanicolaou & Kokkalis (2008) have experimentally evaluated the maximum and steady state penetration depths of vertical fountains to be $3l_M$ and $2l_M$, respectively, with l_M being a characteristic length scale (Fischer *et al.* 1979). In an attempt to predict the terminal penetration depth with a one-dimensional integral model using the above parameters, they showed that model predictions may deviate up to 15% from the observed values. Abraham (1967) has proposed a model to estimate the height of rise of vertical jets issuing in a homogeneous ambient: it predicted a terminal height of rise of $2.06l_M$, which is generally in agreement with the reported heights from several experiments (Turner 1966; Roberts & Toms 1987; Zhang & Baddour 1998; Papanicolaou & Kokkalis 2008). Recently, Jirka (2004) has applied Corjet to predict the height of rise of a vertical fountain issuing into a homogeneous environment. For initially jet-like flows, Corjet predicted the terminal rise height of vertical fountains to be about $2.2l_M$, defined as the sum of axis elevation and the adopted jet visual width $\sqrt{2}b$. Note that the value of b used is not reported, although the computed jet width at this elevation becomes theoretically infinite ($m = 0$).

Corjet has also been applied to dense jets inclined at 60°. The model prediction regarding the terminal height of rise is $1.9l_M$, which is lower than the measured heights

$2.2l_M$ and $2.1l_M$ reported by Roberts & Toms (1987) and Papakonstantis *et al.* (2007), respectively. The predicted centreline dilution at the terminal rise height is $0.29F_o$, where F_o is the jet densimetric Froude number (Fischer *et al.* 1979) that is lower than $0.38F_o$ measured by Roberts & Toms (1987). Besides, comparison of Corjet results for the trajectory of a 55° inclined jet with the experimental data of Hutter & Hofer (1978) show that the model underestimates the outer, visual jet boundary (maximum rise height and distance from the point of impingement) by approximately 15%.

Furthermore, Corjet has been applied to estimate the maximum and terminal height of rise of vertical round jets and plumes in a linearly density-stratified ambient fluid. The agreement between experiments and predictions for initially plume-like flows has been found to be satisfactory (Wong & Wright 1988; Konstantinidou & Papanicolaou 2003; Jirka 2004). However, for jets Corjet predicted a maximum height of rise (sum of centreline elevation and visual width $\sqrt{2}b$) of $3.3l_j$ and a mean horizontal spreading elevation of about $1.5l_j$, with l_j being the characteristic length scale for jets in a stratified environment (Fischer *et al.* 1979). The corresponding measured elevations by Wong & Wright (1988) are $3.6l_j$ and $2.6l_j$, while those by Konstantinidou & Papanicolaou (2003) are $3.55l_j$ and $(2–2.5)l_j$. Although the maximum height of rise seems to be underestimated by approximately 10%, the deviation is considerable (30–40%) for the spreading elevation and consequently for the average dilution.

In summary, the attempts to simulate negatively buoyant jets using the parameters measured in positively buoyant ones usually underestimate (i) the maximum rise height and spreading elevation in a linearly stratified ambient and (ii) the maximum rise height and the corresponding dilution, as well as the distance from the point of impingement in inclined jets in homogeneous ambient, if compared to available experimental data.

A possible reason for the deviations between models and measurements may be attributed to the values of the entrainment coefficient. Higher entrainment coefficients in jet-like flows result in higher dilution rates and consequently in lower heights of rise. Kaminski, Tait & Carazzo (2005) have stated that the entrainment is significantly reduced in flows with negative buoyancy if compared to that in simple jets. However, their study does not rely on measurements of velocity distributions. From experiments they have inferred a reduced entrainment coefficient, using the analytical expression proposed by Woods & Caulfield (1992). A value of 0.057 ($\approx 0.04\sqrt{2}$, top-hat formulation) is used to match their experimental results regarding the volume flux which corresponds to the threshold between buoyant convection and partial collapse to a fountain. Kaminski *et al.* have also proposed an expression for the entrainment coefficient similar to that of Priestley & Ball (1955), which contains an extra nonlinear term modifying the first term α_j in (1). Carazzo, Kaminski & Tait (2006) have evaluated the terms introduced in that expression, using the data regarding only positively buoyant jets.

In the present work, it is shown that experimentally observed parameters regarding the steady state (terminal) or spreading heights in flows with negative or reversing buoyancy, as well as the distance from the point of impingement for discharges at an angle and the corresponding dilutions, can be obtained using significantly lower values of the jet entrainment coefficient than that of a simple jet, $\alpha_j \approx 0.055$ (Fischer *et al.* 1979; List 1982; Papanicolaou & List 1988). The flows under investigation are initially momentum-driven (jet-like); i.e. their initial Richardson number is very small.

2. Integral model and dimensional arguments

2.1. *Description of the integral model*

A definition diagram for three separate cases of negatively buoyant jets is given in figure 1. The time-averaged Reynolds equations of motion are written in cylindrical polar coordinates (s, r), assuming that s measures the distance along the axis and that r is perpendicular to the jet axis, while θ is the local angle of jet axis to the horizontal (figure 1*b*); u is the velocity component in the s direction; g is the gravitational acceleration and ρ_a the ambient fluid density. Assuming that the pressure deviation from a hydrostatic distribution within the jet is neglected, and the Boussinesq approximation is valid, the volume flux, the specific momentum and buoyancy fluxes over a jet cross-section A perpendicular to the axis are (List 1982)

$$\mu(s) = \int_A u(r, s)\,\mathrm{d}A = \int_0^\infty u(r, s) 2\pi r\,\mathrm{d}r, \tag{4}$$

$$m(s) = \int_A u^2(r, s)\,\mathrm{d}A = \int_0^\infty u^2(r, s) 2\pi r\,\mathrm{d}r, \tag{5}$$

$$\beta(s) = \int_A g\frac{[\rho_a - \rho(r, s)]}{\rho_a} u(r, s)\,\mathrm{d}A = \int_0^\infty g\frac{[\rho_a - \rho(r, s)]}{\rho_a} u(r, s) 2\pi r\,\mathrm{d}r. \tag{6}$$

In the above equations the cross-sectional area A is considered to be circular; ρ is the jet density, and $g' = g(\rho_a - \rho)/\rho_a$ is the effective gravitational acceleration.

The mean velocity and excess or deficiency density profiles are assumed to be Gaussian (Jirka 2004):

$$u = u_c \exp(-r^2/b^2) \quad \text{and} \quad g' = g'_c \exp -[r^2/(\lambda b)^2], \tag{7}$$

where λ is the concentration to velocity 1/e–width ratio, and c denotes centreline values. Using the local variables $\mu = \pi b^2 u_c$, $m = \pi b^2 u_c^2/2$ and $\beta = \pi b^2 u_c g'_c \lambda^2/(\lambda^2 + 1)$ in (4)–(7), the volume, momentum and buoyancy conservation equations of a turbulent buoyant jet in a density-stratified ambient with buoyancy frequency N, are written as follows:

$$\frac{\mathrm{d}\mu}{\mathrm{d}s} = 2\sqrt{2\pi}\alpha m^{1/2}; \tag{8}$$

$$\frac{\mathrm{d}m}{\mathrm{d}s} = \frac{1 + \lambda^2}{2}\frac{\mu\beta}{m}\sin\theta; \tag{9}$$

$$\frac{\mathrm{d}\theta}{\mathrm{d}s} = \frac{1 + \lambda^2}{2}\frac{\mu\beta}{m^2}\cos\theta; \tag{10}$$

$$\frac{\mathrm{d}\beta}{\mathrm{d}s} = \mu\frac{g}{\rho_\alpha}\frac{\mathrm{d}\rho_\alpha}{dz}\sin\theta = -\mu N^2\sin\theta. \tag{11}$$

The geometry of the jet trajectory is defined as

$$\frac{\mathrm{d}x}{\mathrm{d}s} = \cos\theta, \tag{12}$$

$$\frac{\mathrm{d}z}{\mathrm{d}s} = \sin\theta. \tag{13}$$

The set (8)–(13), hereafter referred to as the Gaussian model, is based on the model formulation by Fan (1967) for inclined, round buoyant jets. However, making a top-hat assumption regarding the cross-sectional velocity and excessive or deficient density

distribution, (8)–(10) can be written as

$$\frac{\mathrm{d}\mu}{\mathrm{d}s} = 2\sqrt{\pi}\alpha m^{1/2}, \tag{14}$$

$$\frac{\mathrm{d}m}{\mathrm{d}s} = \frac{\mu\beta}{m}\sin\theta, \tag{15}$$

$$\frac{\mathrm{d}\theta}{\mathrm{d}s} = \frac{\mu\beta}{m^2}\cos\theta, \tag{16}$$

where the entrainment coefficient α in Gaussian modelling has been replaced by $\alpha\sqrt{2}$ in top-hat modelling and (8)–(10) by (14)–(16).

The set of six nonlinear differential equations is an initial-value problem, and it can be solved numerically (using for example a fourth-order Runge–Kutta routine), if the entrainment coefficient α and the jet width ratio λ are properly defined. The local entrainment coefficient is evaluated by the expression proposed by Priestley & Ball (1955) (1), and the values proposed by Papanicolaou & List (1988) are used for α_j, α_p and R_p, which respectively are 0.0545, 0.0875 and 0.63. However, the asymptotic plume Richardson number R_p is re-evaluated following the suggestion by Wang & Law (2002). Since the estimated local momentum flux is 10% higher than the momentum computed from the time-averaged velocity profile,

$$R_p = \frac{\mu\beta^{1/2}}{(1.1m)^{5/4}} = \frac{0.63}{(1.1)^{5/4}} = 0.56. \tag{17}$$

This value almost coincides with that proposed by Fischer *et al.* (1979) ($R_p = 0.557$), estimated from the experiments by Rouse, Yih & Humphreys (1952) by taking into consideration only the contribution of the mean kinematical momentum flux. The Richardson number for a local buoyant jet is computed using the absolute value of β, and it cannot be greater than R_p. This results in an entrainment coefficient which does not exceed the plume entrainment coefficient α_p. Therefore, the entrainment coefficient is evaluated by (1) under the restriction $R(s) \leqslant R_p$.

The variable λ has been found to vary between two asymptotic values, λ_j and λ_p, which correspond to jet and plume regimes, respectively. The values reported by Papanicolaou & List (1988) are $\lambda_j = 1.20$ and $\lambda_p = 1.067$. A formulation similar to (2) regarding the entrainment coefficient can be used to compute λ as a function of the local Richardson number of the flow. However, a constant $\lambda = 1.20$ will be used, as it has been indicated to represent an average value over the whole range, from jets to plumes. The variation of λ in negatively buoyant jets is vague, since there is significant uncertainty in the available data, regarding their spreading rate. Moreover, Jirka (2004) has shown that a constant value of λ usually gives good predictions.

The initial conditions will be applied at the virtual jet origin. Following List & Imberger (1973), the virtual-jet origin is located at a distance s_o from the nozzle, defined by $C_p = Q/s_o M^{1/2}$, beyond which self-similarity is implied. Papanicolaou & List (1982) have evaluated the local jet width parameter C_p as

$$C_p = \frac{\mu(s)}{m(s)^{1/2}s} = 0.27. \tag{18}$$

Substituting $\mu = Q$ and $m = M$ in (18) (Q and M being the volume and specific momentum fluxes respectively at the source), the virtual jet origin is located at a distance $s_o = \sqrt{\pi/4}/C_p = 3.28d$, d being the jet diameter. Other researchers (e.g. Jirka 2004) have considered the jet origin to be coincidental with the end of the zone of

flow establishment, i.e. at $s_o = 5d$. In the present model we assume the following initial conditions valid at $s_o = 3.28d$:

$$m_o = M, \quad \mu_o = Q, \quad \beta_o = B \quad \text{and} \quad \theta_o = \Theta, \tag{19}$$

where B is the specific buoyancy flux at the source; Θ is the angle of inclination to the horizontal at the source, and the subscript 'o' denotes values at the virtual origin. It should be noted that if we consider s_o to be equal to $5d$, then the initial volume flux must be modified. Assuming that $m_o = M$ (momentum conservation), from (19) and $\mu_o = Q\sqrt{2}$ (Jirka 2004) one can obtain $s_o \cong 5d$.

The derivation of the above integral formulation is similar to that of previous integral models, predominantly developed to simulate positively buoyant jets (Fan 1967). The model predictions are subsequently compared to available experimental data regarding the jet geometry and dilution.

2.2. *Dimensional analysis and theoretical considerations*

Let us consider a buoyant jet of density ρ_o, discharging vertically in an infinite volume of calm ambient, with a linear density gradient $\mathrm{d}\rho_a/\mathrm{d}z$. The buoyancy frequency N (with dimensions T^{-1}) is defined as

$$N^2 = -\frac{g}{\rho}\frac{\mathrm{d}\rho_a}{\mathrm{d}z}. \tag{20}$$

If U is the uniform velocity at the source and ρ_a the local ambient fluid density, then the initial volume flux and the specific (per unit mass) momentum and buoyancy fluxes are defined as

$$Q = UA, \quad M = QU \quad \text{and} \quad B = g'_o Q, \tag{21}$$

respectively. The effective gravitational acceleration $g'_o = g(\rho_a - \rho_o)/\rho_a$ can be either positive ($\rho_a > \rho_o$) or negative ($\rho_a < \rho_o$). Two length scales based upon the initial kinematic buoyant jet characteristics are defined as (Fischer *et al.* 1979)

$$l_Q = \frac{Q}{M^{1/2}} \quad \text{and} \quad l_M = \frac{M^{3/4}}{B^{1/2}}, \tag{22}$$

the ratio of which is defined to be the initially buoyant jet Richardson number

$$R_o = \frac{l_Q}{l_M} = \frac{QB^{1/2}}{M^{5/4}} = \left(\frac{\pi}{4}\right)^{1/4}\frac{\sqrt{g'_o d}}{U}. \tag{23}$$

R_o is inversely proportional to the initial jet densimetric Froude number $F_o = U/\sqrt{g'_o d}$. When the initial momentum flux M is dominant, $R_o \to 0$ ($F_o \to \infty$), the jet is momentum driven.

The vertical penetration depth Z of negatively buoyant jets discharging at an angle Θ with respect to the horizontal depends upon the variables characterizing the source conditions. Ignoring viscosity (as the jet is assumed to be turbulent) and the effect of the initial volume flux Q ($\mu \gg Q$ far from the source), a general functional relationship for the dependent variable Z is

$$Z = f(M, B, N, \Theta). \tag{24}$$

(a) In the case of a negatively buoyant jet at an angle Θ in a uniform ambient shown in figure 1(a,b), (24) is written as $Z = f(M, B, \Theta)$ leading to (Turner 1966)

$$\frac{Z}{l_M} = C_1(\Theta), \tag{25}$$

where the normalized maximum penetration height is constant for each angle Θ. In a similar manner the horizontal distance to the point of impingement X_i reads

$$\frac{X_i}{l_M} = C_2(\Theta). \tag{26}$$

According to Roberts & Toms (1987), if $R_o \to 0$ the dilution at the jet axis $S_c = \Delta\rho_o/\Delta\rho_c(s)$, $\Delta\rho_o = \rho_\alpha - \rho_o$, $\Delta\rho_c = \rho_\alpha - \rho_c(s)$, is normalized as

$$\frac{S_c}{F_o} = C_3(\Theta). \tag{27}$$

(*b*) For a vertical positively buoyant jet in a linearly density-stratified ambient shown in figure 1(*c*), (24) is written as $Z = f(M, B, N)$, leading to the relationship (Wong & Wright 1988; Konstantinidou & Papanicolaou 2003)

$$\frac{Z}{l_j} = f\left(\frac{M}{B}N\right), \quad l_j = \frac{M^{1/4}}{N^{1/2}}. \tag{28}$$

For an initially simple jet ($B \to 0$) the normalized terminal rise height Z_m and spreading elevation Z_s are written as

$$\frac{Z_m}{l_j} = C_4 \quad \text{and} \quad \frac{Z_s}{l_j} = C_5. \tag{29}$$

If the rise heights are normalized by the length scale l_M then (29) may be written as

$$\frac{Z_m}{l_M} = C_4\left(\frac{MN}{B}\right)^{-1/2} \quad \text{and} \quad \frac{Z_s}{l_M} = C_5\left(\frac{MN}{B}\right)^{-1/2}.$$

The mean elevation of lateral spreading Z_s can be computed from the buoyancy conservation equation at Z_m, assuming no further mixing of the jet with ambient fluid during its descent from Z_m to Z_s. At Z_m the buoyancy flux is

$$\beta(Z_m) = \frac{\overline{\Delta\rho}}{\rho_o} g\mu(Z_m); \quad \overline{\Delta\rho} = \overline{\rho} - \rho_\alpha(Z_m), \tag{30}$$

with the overbar denoting the average density over the jet cross-section. Then, substituting $\overline{\Delta\rho}$ from (30) into (20) one can compute the distance Δz below Z_m where the buoyancy of the reversing flow (assuming no further mixing with ambient fluid) becomes neutral. This is the mean jet spreading elevation Z_s computed from

$$N^2 = -\frac{g}{\rho_o}\frac{\overline{\Delta\rho}}{\Delta z} \Rightarrow \Delta z = Z_s - Z_m = -\frac{g}{\rho_o}\frac{\overline{\Delta\rho}}{N^2} = \frac{\beta(Z_m)}{N^2\mu(Z_m)}. \tag{31}$$

All the above jets disperse with negative buoyancy, relative to the direction of movement. In case (*b*) though, the jet is slightly positively buoyant at the nozzle elevation, but it becomes negatively buoyant almost immediately if $MN/B \gg 1$ (Wong & Wright 1988; Konstantinidou & Papanicolaou 2003). Then it climbs up to the elevation Z_m, where the momentum flux vanishes, and descends to the neutral buoyancy elevation Z_s, where it spreads laterally.

3. Experimental data for comparison

In this section, we will briefly describe the experiments performed by the authors of this paper and presented elsewhere, from which data are taken for comparison.

In addition, comparisons are made with results of other investigators, as discussed in the next section.

Data regarding vertical buoyant axisymmetric jets in a linearly density-stratified calm ambient were obtained by Konstantinidou & Papanicolaou (2003). The experiments were carried out in a linearly stratified tank with dimensions 1.00×0.60 m and 0.80 m deep. Reynolds numbers at the source were in the range $1000 < Re < 5200$, while the initial jet Richardson number varied from 0.007 to 0.4. They cover the full range, from jets (small initial density difference between jet and ambient and large momentum) to plumes (initial buoyancy flux being dominant compared to the momentum); i.e. they extend in the range $0.1 < MN/B < 150$ (see appendix B, table 2).

Data for vertical negatively buoyant jets issuing into a homogeneous ambient were obtained by Papanicolaou & Kokkalis (2008) in a tank of dimensions 0.80×0.80 m and 1.00 m deep, for buoyancy-preserving (saltwater) jets, over a wide range of initial Richardson numbers (0.02 to 0.1; see appendix B, table 3). The jets were turbulent from the source (with the Reynolds numbers in the range $830 < Re < 5800$), as the transition to turbulence occurred naturally within five jet diameters.

Experiments regarding the terminal height of rise of inclined dense jets in a homogeneous ambient have recently been reported by Papakonstantis *et al.* (2007). Further analysis of those experiments has provided data regarding the distance from the point of impingement. The tank used had the horizontal dimensions 3.0×1.5 m and is 1 m deep. The jet pipe of diameter 0.6 cm was inclined at 45°, 60° and 75° with respect to the horizontal. Reynolds numbers at the source exceeded 6000, while the initial jet Richardson number varied from 0.015 to 0.039 ($24 \leqslant F_o \leqslant 63$). The experimental conditions are shown in table 4, in appendix B. The measured lengths were corrected for errors introduced from (i) the grid drawn in the front glass panel and not in the centre of the tank where the jet evolves, (ii) the camera position and (iii) the refractive index changes from air to glass to water. The correction procedure is presented in appendix A.

4. Comparison of computed parameters with experiments

The data from the experiments mentioned in the last section are compared to the Gaussian and the top-hat model predictions regarding the trajectory and the dilution.

4.1. *Vertical jet in a linearly stratified ambient*

The results of the models are first compared to the data of Konstantinidou & Papanicolaou (2003), shown in figure 2, regarding the maximum height of rise and spreading elevation of a jet issuing in a linearly density-stratified environment. From figure 2 it is seen that for large values of MN/B (>10) the measured maximum normalized rise height Z_m/l_j takes a value of 3.5 to 3.6, while the average spreading elevation data have substantial scatter in the range $2 < Z_s/l_j < 2.5$. When the flow is initially plume-like ($MN/B \ll 1$), both models predict the experimental findings quite accurately. This flow is positively buoyant for most of its vertical path. When the flow is initially jet-like ($MN/B \gg 1$), though, both models underestimate the normalized maximum height of rise and spreading elevation of the jet considerably. This flow is negatively buoyant for most of its vertical path. The Gaussian model has predicted $Z_m/l_M = 2.55$ and $Z_s/l_M = 1.33$, while the top-hat model predicted $Z_m/l_M = 2.65$ and $Z_s/l_M = 1.39$. These values are lower than the measured ones $Z_m/l_M = 3.55$

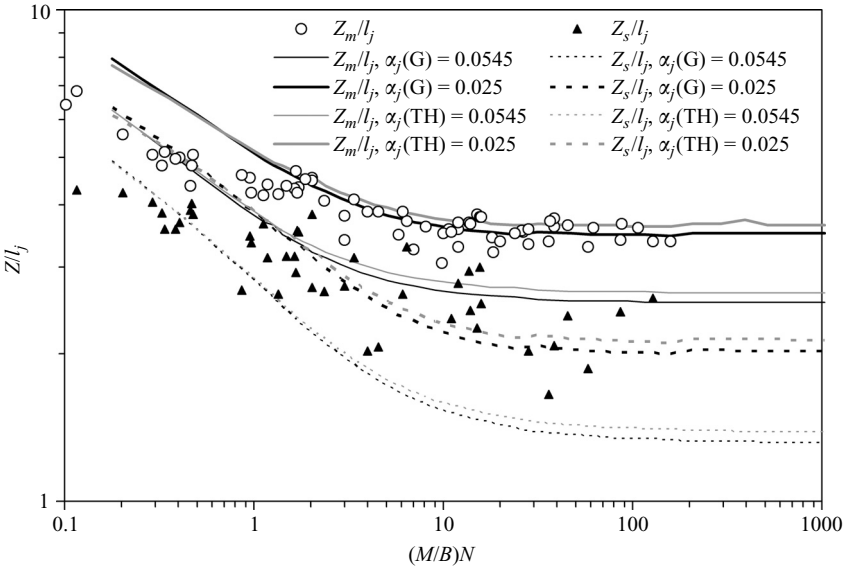

FIGURE 2. Comparison of model predictions with experiments by Konstantinidou & Papanicolaou (2003) for the normalized maximum height of rise and mean spreading elevation of vertical buoyant jets issuing in density-stratified fluid. G represents Gaussian and TH top-hat predictions.

and $Z_s/l_M = 2.25$, Z_m being the elevation where the momentum vanishes. It is noted that the jet width $\sqrt{2}b$ or b (in Gaussian and top-hat modelling respectively) has not been added to the computed elevation.

Good agreement with the measured normalized maximum height of rise and spreading elevation of a jet ($MN/B \gg 1$) issuing in a linearly density-stratified environment was obtained by reducing the jet entrainment coefficient α_j from 0.0545 to 0.025 as shown in figure 2. (The values of α_j must be multiplied by $\sqrt{2}$ in top-hat modelling.) The predicted normalized elevation of vanishing momentum Z_m/l_M and lateral spreading Z_s/l_M are 3.66 and 2.13 for top-hat and 3.50 and 2.02 for Gaussian modelling, respectively. These results compare well with the experimental data of Konstantinidou & Papanicolaou (2003), as shown in figure 2, and the measurements by Wong & Wright (1988), mentioned in the introduction.

It is concluded that if we reduce the jet entrainment coefficient of a vertical jet ($MN/B \gg 1$) issuing into a linearly stratified fluid, we can obtain the maximum rise height predicted by experiments without having to add the jet width to the elevation where the momentum vanishes, as proposed in Corjet. In addition, the computed spreading elevation, which after all is the important parameter indicative of the dilution obtained, is quite close to the experimental value, whereas it is underestimated by about 30% by Corjet (Jirka 2004). Lower spreading elevations indicate an increased rate of mixing, attributed to the higher jet entrainment coefficient applied. A deviation of the same order is obtained regarding the maximum height of rise without adding the term $\sqrt{2}b$ to the computed centreline elevation. This may indicate that the width $\sqrt{2}b$ should not be added to the predicted maximum height in vertical jets.

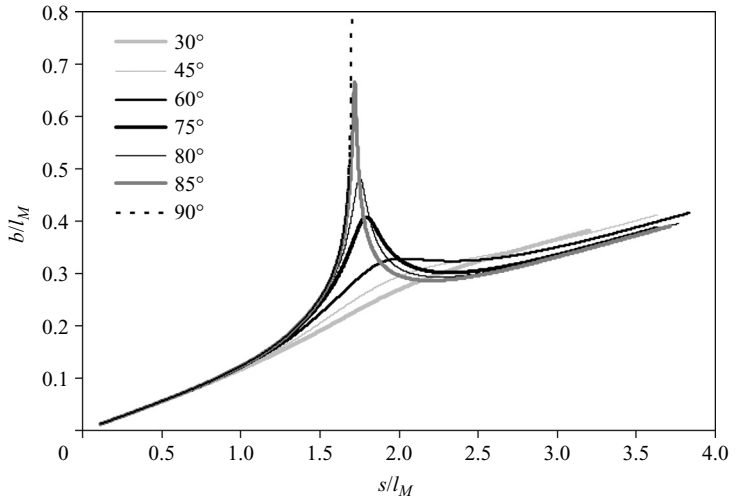

FIGURE 3. Computed normalized jet width b/l_M versus the dimensionless distance s/l_M from the origin of dense jets inclined at different angles.

4.2. *Inclined and vertical jets in a homogeneous ambient*

The trajectory and the visual boundaries of inclined negatively buoyant jets in a uniform ambient were computed using both Gaussian and top-hat velocity and excess density distributions and are subsequently compared to experimental data (Papakonstantis *et al.* 2007; Papanicolaou & Kokkalis 2008). The jet trajectory is assumed to be that of the centreline. The visual boundaries are computed by adding the perpendicular jet width $\sqrt{2}b$ (or b in top-hat modelling), on each side of the jet trajectory (Jirka 2004). The experiments by Papakonstantis *et al.* (2007) provide data regarding only the visual jet boundaries and not the centreline trajectory. Evaluation of the appropriate jet width b is critical for the model performance, and therefore it is pertinent to examine the behaviour of the computed jet width in momentum-driven flows.

A jet with initial Richardson number $R_o \approx 0.03$ ($F_o \approx 32$) is studied for inclination angles of 30°, 45°, 60°, 75°, 80°, 85° and 90° (vertical), using the Gaussian formulation. In figure 3 the normalized computed jet width b/l_M is plotted against the normalized trajectory s/l_M, s being the trajectory length from the jet origin. One may clearly note the nonlinear growth of the jet width with s. At inclination angles $\Theta < 60°$, the growth of the jet width ($1.5 < s/l_M < 2.5$) is quite smooth. At higher inclination angles ($\Theta > 60°$), the computed jet width around the inflection point (maximum centreline elevation on which the vertical momentum vanishes) grows rapidly and becomes quite large, then decreases also rapidly after that point and grows again smoothly for $s/l_M > 2.5$. When the jet is vertical its width attains the highest growth rate. However, as observed from our experiments, the large-scale structures increase monotonically along the jet trajectory. Therefore, the computed jet width around the inflection point should be limited by a value allowing its monotonic growth. From figure 3 it is evident that around the maximum rise height, the jet width cannot exceed a limiting value of about $0.3l_M$. Jirka (2004) reports that Corjet predicts terminal heights equal to $1.9l_M$ and $2.2l_M$ for inclined jets at angles of 60° and 90° (vertical jet), respectively. These results correspond to a jet width approximately equal to $0.39l_M$ (visual width

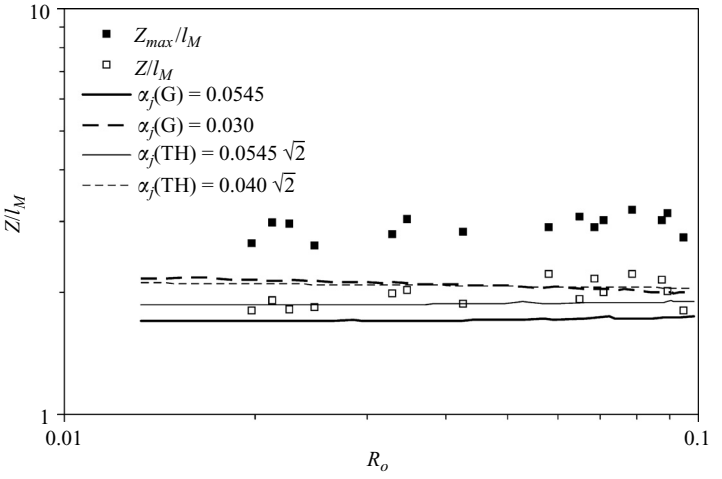

FIGURE 4. Comparison of model predictions with experiments by Papanicolaou & Kokkalis (2008), for the maximum and terminal (steady state) penetration depths of vertical dense jets issuing into homogeneous ambient. G represents Gaussian and TH top-hat predictions.

$b\sqrt{2} = 0.39\sqrt{2}l_M$) in both cases. However, the corresponding computed jet widths are found to be $0.31l_M$ and l_M for 60° and 90° (vertical jet) respectively, as shown in figure 3. Similar jet width behaviour is observed when the top-hat formulation is employed. The limiting value of the jet width is $0.47l_M \approx 0.3\sqrt{2}l_M$.

Therefore, in the computations which follow regarding the maximum elevation of the upper jet boundary (terminal height of rise), the width added to the maximum centreline elevation is chosen as follows: (i) when $\Theta \leqslant 60°$, b is the computed jet width $b(s) = \mu(s)/[2\pi \mathrm{m}(s)]^{1/2}$; (ii) when $\Theta > 60°$, $b = 0.3l_M$ and $0.47l_M$ for Gaussian and top-hat modelling respectively; and (iii) for $\Theta = 90°$, $b = 0$ (see §4.1). The jet boundaries beyond the terminal rise height ($s/l_M < 1.5$ and $s/l_M > 2.5$) are obtained using the computed jet width $b(s)$.

The data of Papanicolaou & Kokkalis (2008) are compared to the model results for vertical initially jet-like flows ($R_o < 0.1$) in figure 4. The normalized measured maximum and terminal penetration depths take the values $Z_{max}/l_M = 3$ and $Z/l_M = 2$ respectively. Using the conventional jet entrainment coefficient ($\alpha_j = 0.0545$ for the Gaussian model or $\alpha_j = 0.0545\sqrt{2}$ for the top-hat model), the computed, normalized terminal rise height Z/l_M is 1.70 and 1.87 with the Gaussian and top-hat formulations respectively, indicating significant underestimation when compared to the measured values, especially for the Gaussian model. Greater rise height ($Z/l_M \approx 2.10$) is obtained if the jet entrainment coefficient is reduced to 0.030 and $0.040\sqrt{2}$ with the Gaussian and top-hat formulations, respectively. (The latter value has also been proposed by Kaminski *et al.* 2005.)

The experiments by Papakonstantis *et al.* (2007) for 45°, 60° and 75° inclined negatively buoyant jets are simulated, and the computed terminal (steady state) heights of rise are compared to the measured heights in figures 5, 6 and 7, respectively. The Gaussian model (for $\alpha_j = 0.0545$) predicts heights $1.36l_M$, $1.79l_M$ and $2.03l_M$ for Θ equal to 45°, 60° and 75° respectively, values which are lower than the mean measured heights ($1.57l_M$, $2.12l_M$ and $2.47l_M$), showing that the Gaussian model considerably underestimates the height of rise in all cases. On the other hand, the top-hat formulation gave greater heights than the Gaussian one for the same jet

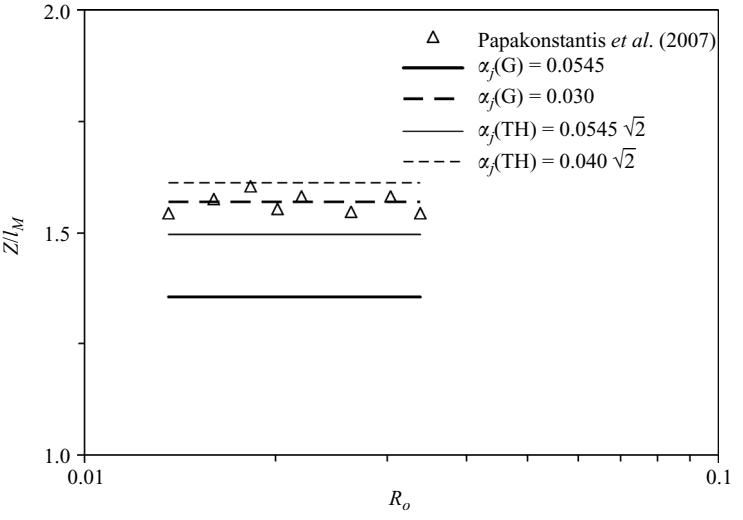

FIGURE 5. Comparison of model predictions with experiments by Papakonstantis *et al.* (2007) for the terminal rise height of 45° inclined dense jets. G represents Gaussian and TH top-hat predictions.

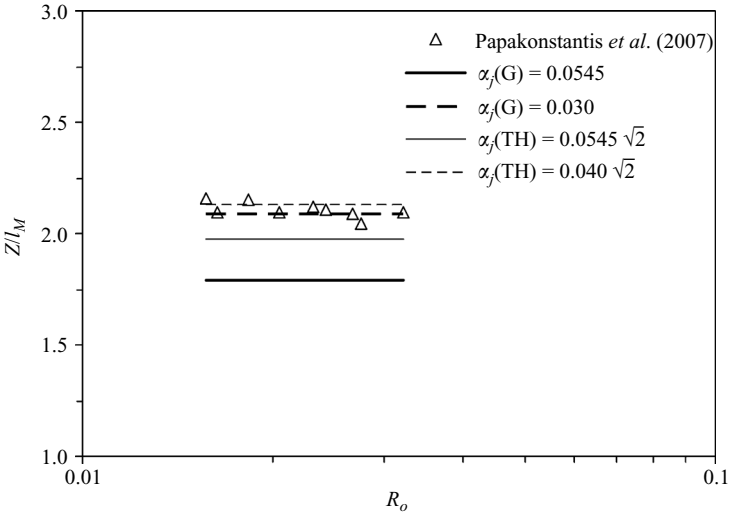

FIGURE 6. Comparison of model predictions with experiments by Papakonstantis *et al.* (2007) for the terminal rise height of 60° inclined dense jets. G represents Gaussian and TH top-hat predictions.

entrainment coefficient, simulating the experimental results more accurately. However, the predictions are still lower than the experimental data (table 1). Using a lower jet entrainment coefficient $\alpha_j = 0.03$ (Gaussian formulation) and $\alpha_j = 0.040\sqrt{2}$ (top-hat formulation) in inclined jets, the measured terminal heights are accurately predicted, as shown in figures 5, 6 and 7.

In summary, the performance of Gaussian modelling regarding the prediction of the terminal rise height is investigated in terms of the jet width b and the angle of inclination Θ, including unpublished data from ongoing experiments by Ilias

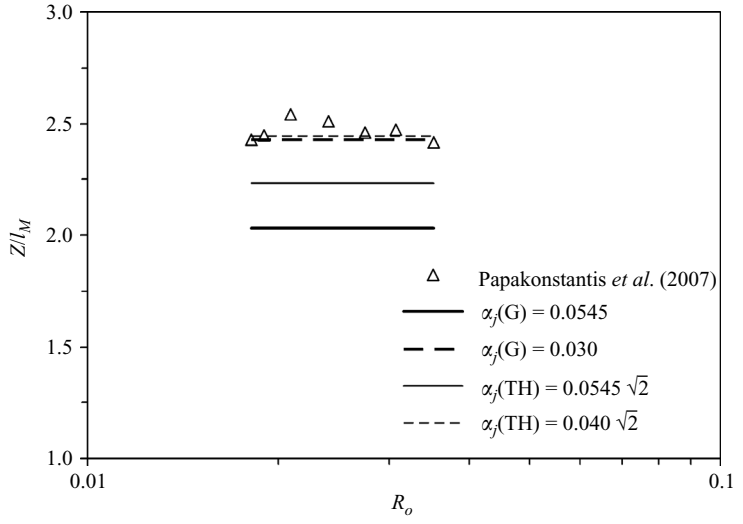

FIGURE 7. Comparison of model predictions with experiments by Papakonstantis *et al.* (2007), for the terminal rise height of 75° inclined dense jets. G represents Gaussian and TH top-hat predictions.

	Gaussian model				Measured
Θ	α_j	Z_c/l_M	b/l_M	$(Z_c + b\sqrt{2})/l_M$	Z/l_M
45°	0.0545	0.98	0.27	1.36	1.57
60°		1.35	0.31	1.79	2.12
75°		1.61	0.30	2.03	2.47
80°		1.66	0.30	2.08	–
85°		1.69	0.30	2.12	2.51
90°		1.70	0.00	1.70	2.00
45°	0.030	1.23	0.23	1.56	1.57
60°		1.68	0.28	2.08	2.12
75°		2.00	0.30	2.42	2.47
80°		2.06	0.30	2.49	–
85°		2.10	0.30	2.53	2.51
90°		2.12	0.00	2.12	2.00
	Top-hat model				Measured
Θ	α_j	Z_c/l_M	b/l_M	$(Z_c + b)/l_M$	Z/l_M
45°	$0.0545\sqrt{2}$	1.08	0.42	1.50	1.57
60°		1.48	0.50	1.97	2.12
75°		1.76	0.47	2.23	2.47
80°		1.82	0.47	2.29	–
85°		1.86	0.47	2.33	2.51
90°		1.87	0.00	1.87	2.00
45°	$0.040\sqrt{2}$	1.21	0.40	1.61	1.57
60°		1.65	0.47	2.12	2.12
75°		1.97	0.47	2.44	2.47
80°		2.03	0.47	2.50	–
85°		2.07	0.47	2.54	2.51
90°		2.09	0.00	2.09	2.00

TABLE 1. Measured and predicted terminal height of rise of jets inclined at different angles.

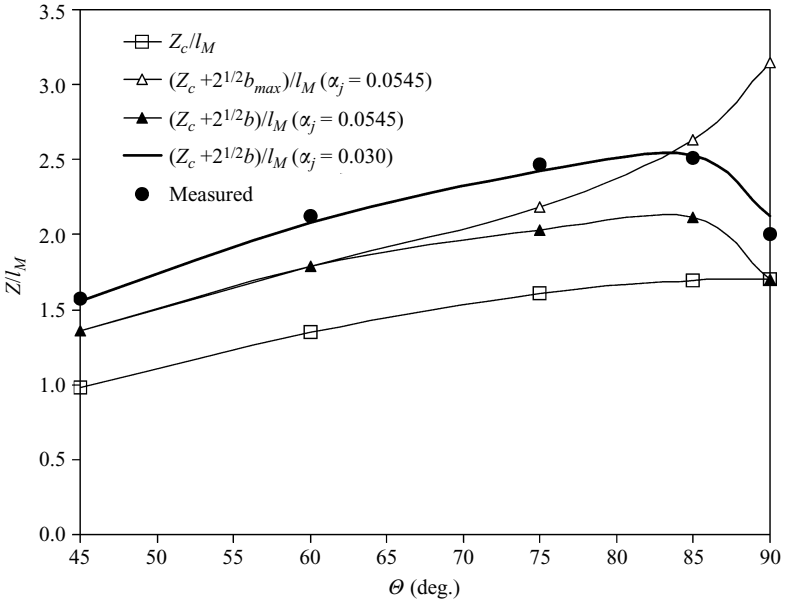

FIGURE 8. Comparison of measurements with terminal rise height predictions for different evaluations of the jet width in dense jets inclined at various angles.

G. Papakonstantis regarding the 85° angle. In figure 8 the following normalized rise heights are plotted as a function of the inclination angle:

$\frac{Z_c}{l_M}$ centreline elevation ($\alpha_j = 0.0545$);

$\frac{Z_c + b_{\max}\sqrt{2}}{l_M}$ maximum rise height, using the computed jet width ($\alpha_j = 0.0545$);

$\frac{Z_c + b\sqrt{2}}{l_M}$ maximum rise height, using $b = 0.30 l_M$ for $60^\circ < \Theta < 90$ ($\alpha_j = 0.0545$);

$\frac{Z_c + b\sqrt{2}}{l_M}$ maximum rise height, using $b = 0.30 l_M$ for $60^\circ < \Theta < 90$ ($\alpha_j = 0.030$).

For $\Theta = 90^\circ$ only the predicted axial elevation is used, as the width grows in the horizontal direction. One may note that if the computed jet width is added to the maximum axis elevation, the model underestimates the terminal height of rise for angles Θ up to about 80°, whereas it overestimates it for greater angles. When an upper bound for the jet width is set ($b = 0.30 l_M$), as discussed previously, then the maximum rise height is systematically lower than the measured one for $\alpha_j = 0.0545$. However, if a reduced value of the jet entrainment coefficient is employed ($\alpha_j = 0.030$), the model predictions are in agreement with the experiments by Papakonstantis *et al.* (2007) for all inclination angles. The model predictions and the corresponding measured values for the terminal height of rise are summarized in table 1.

Detailed data for the jet trajectory have not been reported by Papakonstantis *et al.* (2007). However, analysis of the available experiments has provided the relevant data used in the present work. In figure 9 the model is compared to the experimental data regarding the trajectory of a 45° inclined dense jet with $R_o = 0.0295$ ($F_o = 31.90$). It is evident that the model predictions using the conventional value of the jet entrainment

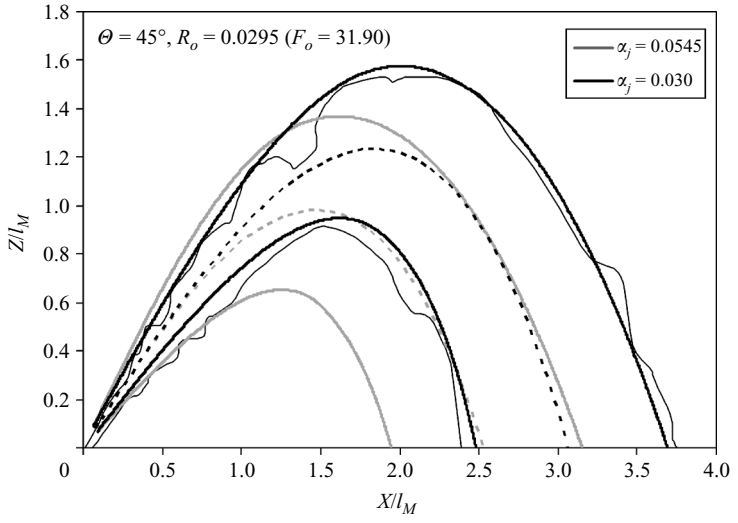

FIGURE 9. Comparison of Gaussian model predictions with experimental data for the trajectory of a 45° inclined dense jet.

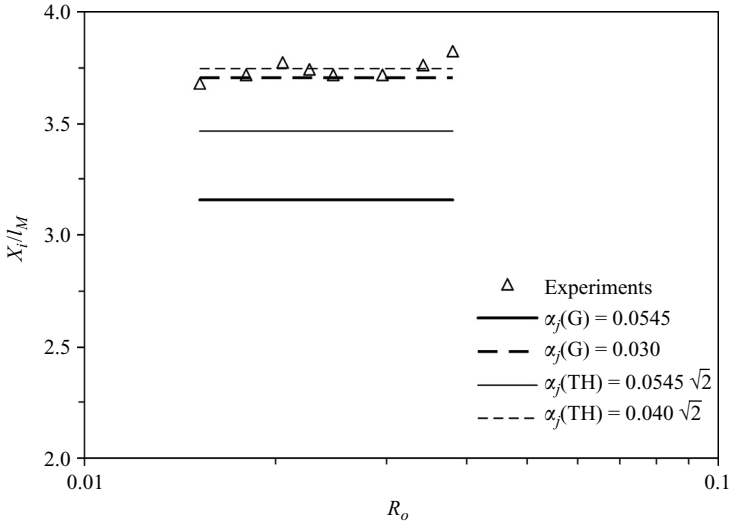

FIGURE 10. Comparison of model predictions with experiments for the horizontal distance to the point of impingement in dense jets inclined at 45°. G represents Gaussian and TH top-hat predictions.

coefficient ($\alpha_j = 0.0545$) diverge from the measured trajectory, whereas if $\alpha_j = 0.030$ is used, model predictions are in agreement with measurements.

Regarding the distance from the point of impingement, comparison of the experimental and numerical results is shown in figures 10 and 11 for inclined jets at 45° and 60°, respectively. Top-hat modelling with $\alpha_j = 0.0545\sqrt{2}$ gives higher values compared to those of the Gaussian one ($\alpha_j = 0.0545$), although both models underestimate considerably the distance X_i to the point of impingement. If the reduced values of the jet entrainment coefficient used above are employed, the predictions of the distance X_i are in agreement with measurements for $\Theta = 45°$ but continue to

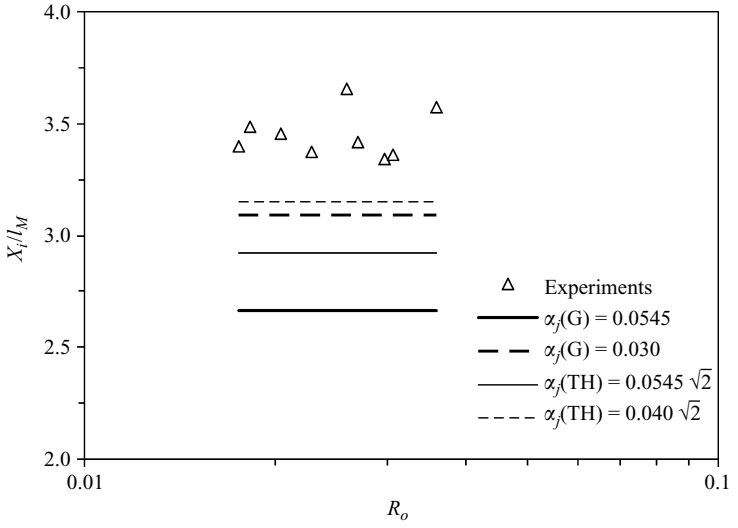

FIGURE 11. Comparison of model predictions with experiments for the horizontal distance from the point of impingement in dense jets inclined at 60°. G represents Gaussian and TH top-hat predictions.

deviate from the measurements for $\Theta = 60°$. However, model prediction regarding the location of the jet axis at the point of impingement is congruent with the value measured by Roberts *et al.* (1997), $X_c = 2.55 l_M$, which is also predicted by Gaussian and top-hat modelling for $\alpha_j = 0.030$ and $\alpha_j = 0.040\sqrt{2}$, respectively.

Dilution measurements in inclined dense jets at 60° have been reported by Roberts & Toms (1987). The measured centreline time-averaged dilutions S_t (at the terminal height of rise) and S_i (at the point of impingement) are $0.38F_o$ for $F_o > 25$ and $1.03F_o$ for $F_o > 12$, respectively. The Gaussian model (for $\alpha_j = 0.0545$) applied for $F_o \cong 26$ predicts $S_t = 0.35F_o$ and $S_i = 0.84F_o$. Although the height of rise is considerably underestimated, the dilution is well predicted. However, the dilution at the point of impingement is substantially underestimated.

If a lower value α_j (0.030) is used, the model predicts $S_t = 0.32F_o$ for the same initial Froude number, showing that the dilution at the terminal height of rise decreases, since the rate of entrainment in the jet regime is lower. However, the dilution at the point of impingement of the centreline increases ($S_i = 0.92F_o$), since the trajectory has been elongated, and it is in satisfactory agreement with that measured by Roberts & Toms (1987). Top-hat modelling can only predict the average dilution; therefore comparison with measurements would be invalid.

5. Discussion

For the calculation of the spreading elevation of jets in linearly density-stratified ambient, re-entrainment has been neglected. A jet with zero or slightly positive buoyancy at the source, issuing in a linearly density-stratified fluid, reaches the terminal height, and it subsequently but slowly returns to the spreading elevation, entraining mostly mixed fluid from the wastefield. After steady state has been reached the overshoot of the jet above the top boundary is quite small, and further mixing

while descending is considered to be negligible. Jets with initially slightly positive or negative buoyancy have the same asymptotic behaviour as pure jets, i.e. for $(M/B)N > 10$.

So far, in inclined jets we have considered the terminal height of rise to be the sum of the maximum trajectory elevation and the jet width b for top-hat modelling. For Gaussian modelling, the width is multiplied by $\sqrt{2}$ (Jirka 2004). In vertical jets the visual width has not been added to the predicted axis elevation. The large-scale structures in round jets or plumes have a diameter that is approximately twice the size of their visual width, i.e. $2\sqrt{2}b$. In an inclined jet, the sequence of large-scale structures determines the upper and lower jet visual boundaries with respect to the axis. The maximum elevation of the upper boundary can be obtained by adding half the size of the large-scale structures ($\sqrt{2}b$) to the local maximum height of the jet axis. However, in a vertical fountain, the sequence of large-scale structures may be noted as a result of the fluctuating elevation of vanishing momentum. Moreover the lateral spreading of the jet boundaries is in the horizontal direction, i.e. normal to the height. Therefore, the term ($\sqrt{2}b$) does not have to be added to the elevation where $m = 0$. The comparison with the experimental data regarding the maximum height of rise and the spreading elevation of a jet issuing into a stratified environment has showed that this approach is valid.

The computed jet width around the terminal rise height (point of inflection of jet trajectory) was investigated and found to increase dramatically for $\Theta > 60^\circ$ and become theoretically infinite at 90° (vertical jet). The jet width is a measure of the 'radius' of the large-scale structures, as they evolve towards the terminal elevation (of vanishing vertical momentum). At large initial inclination angles though, the large-scale jet structures start to collapse around the terminal elevation, where they become wider and flatter. However, pairing of two subsequent large-scale structures cannot produce one that grows explosively. In the vertical jet, the computed normalized width was found equal to l_M, while the observed visual jet width at the terminal rise height from the experiments by Papanicolaou & Kokkalis (2008) does not exceed $0.4l_M$. Similar observations have been made for jets inclined at lower angles. Consequently, in inclined jets at angles $\Theta > 60^\circ$, the calculations indicate that when $1.5 < s/l_M < 2.5$ a limiting value of approximately $0.3l_M$ should be considered for Gaussian modelling and approximately $0.47l_M$ for top-hat modelling. These values are the upper limits of the width in $1.5 < s/l_M < 2.5$, so that monotonic growth is maintained.

Top-hat modelling has generally provided better predictions than the Gaussian one, a result that does not generally agree with the findings in positively buoyant jets. This is true whether a constant or a variable value (between λ_j and λ_p) of λ is used. Varying λ according to an expression similar to that employed for the entrainment coefficient, (1) or (2), the differences in computed rise heights are not significant (less than $0.10l_M$). Consequently, the question that arises is whether a Gaussian distribution of the time-averaged velocity and excess density is appropriate. In positively buoyant jets the maximum time-averaged local effective gravitational acceleration is located at the jet 'core,' within a width b from its axis. Thus the jet core is continuously accelerating, because of the concentrated local force there, resulting in a Gaussian velocity distribution. In other words we may state that if the effective gravity is in phase (acting on the same direction) with velocity, the distribution of the latter is Gaussian, since the shear around the boundaries of large-scale structures results in lateral momentum transfer. In negatively buoyant jets though, the strongest effective gravity around the axis locally decelerates the moving fluid. Assuming initially a

Gaussian velocity distribution in a jet with negative buoyancy (with velocity and effective gravity being out of phase), the strong negative effective gravity in the jet 'core' decelerates the fluid locally faster than the lower effective gravity around the jet boundary. The shear stress between the jet and the ambient fluid is therefore reduced with distance from the origin. This may result in a more 'uniform' velocity distribution that is closer to top hat than to Gaussian, explaining why the computations using top-hat modelling give predictions that are closer to the measurements. However, measurements of the velocity and concentration profiles across the jet are required in order to clarify the form of the distribution.

Regarding the elevation where the initial conditions are applied, experimental observations indicate that the virtual origins of vertical negatively buoyant jets as well as jets in linear stratification are quite close to the source. Assuming that the virtual origin is located at the source ($z_o = 0$), the prediction of Z/l_M is not any different from the case in which $z_o = 3.28d$. However, the numerical results fit the experimental data better for $z_o = 3.28d$, a value that is compatible with the theory by List & Imberger (1973).

In the entrainment modelling a sophisticated (implicit) formula proposed by Kaminski *et al.* (2005) and evaluated by Carazzo *et al.* (2006) could also be used. However, the (explicit) expression proposed by Priestley & Ball (1955) is sufficient for the purpose of the paper, and it is also easier to use.

A question to be answered is why the entrainment coefficient is reduced in negatively buoyant jets. A jet can be modelled as a sequence of sinks along its axis, each of them sucking fluid from a slice of thickness Δs normal to the axis. The rate of entrainment at distance s from the origin is proportional to the strength of the local sink, resulting in a negative pressure gradient in the radial direction. If a jet is momentum-driven (not much change in initial jet momentum) one may note the following:

(i) In positively buoyant jets the buoyancy accelerates the 'core' of the jet, thus increasing the sink strength, since the radial pressure gradient becomes steeper. The rate of entrainment keeps increasing, up to the point of equilibrium (plume-like flow), where it attains a constant value.

(ii) In negatively buoyant jets, the out of phase, negative buoyancy decelerates the jet 'core,' thus reducing the radial pressure gradient and consequently the strength of the local sink. Therefore, the rate of entrainment will be reduced, compared to that of simple jets. Experimental evidence presented in this paper suggests values of 0.030 and 0.025 for negatively buoyant jets in homogeneous and linearly stratified ambient respectively.

For top-hat modelling, the present results show that good agreement with experiments is obtained for a value of $\alpha_j = 0.040\sqrt{2}$, which is considerably lower than the value commonly used for positively buoyant jets ($\alpha_j = 0.0545\sqrt{2} \approx 0.077$) and close to that suggested by Kaminski *et al.* (2005). The reason why different values for α_j are found appropriate for Gaussian and top-hat formulations, in contrast to positively buoyant jets, requires further investigation.

6. Conclusions

Integral one-dimensional modelling is a valuable tool for simulating turbulent buoyant jets. Gaussian and top-hat modelling were employed to simulate negatively buoyant flows which initially are momentum-driven; i.e. their initial Richardson number R_o is very low. When the buoyancy is reversing or acting against the direction

of the flow, the main geometrical parameters and dilution are underestimated if conventional values for the jet entrainment coefficient are used. Top-hat modelling seems to give better predictions than the Gaussian one, pointing out the need for experimental verification of the shape of velocity and concentration distributions in such flows.

Comparison of the model with experimental data regarding the trajectory and mainly the rise heights of inclined and vertical negatively buoyant jets in a homogeneous or linearly stratified ambient, as well as the distance from the point of impingement and the corresponding centreline dilution in inclined negatively buoyant jets in a uniform environment, showed improved model performance when a lower value of the jet entrainment coefficient was employed. The value of this coefficient in a homogeneous calm ambient was found to be about 0.030 and $0.040\sqrt{2}$ for Gaussian and top-hat modelling respectively, while a somewhat lower value of α_j (0.025) was required to predict the maximum height and spreading elevation in vertical jets issuing in a linearly stratified fluid.

In summary, it is indirectly concluded that in jets with negative buoyancy, the entrainment in the momentum-driven flow regime is significantly reduced. Since a higher entrainment rate results in higher dilution rates, proper evaluation of the entrainment coefficient is very important for the simulation of such flows. Experimental investigation for the direct evaluation of the entrainment in negatively buoyant jets via extensive velocity measurements is required.

The support to I. G. P. through a PhD grant from the research committee of the National Technical University of Athens is gratefully acknowledged.

Appendix A. Correction procedure for the measured lengths

The length measurements were obtained using the jet image and the grid drawn in the front glass panel of the dispersion tank. Therefore, the lengths observed on the grid are different than the actual ones, because of the distance of the jet axis plane from the glass and the differences in the refractive index between air and water. If the normal distance between the camera and the front glass panel (where the grid is drawn) at point $(x, z) = (0, 0)$ is Y, then a reading (x_g, z_g) on the grid must be converted to real jet coordinates (x, z) by adding the correction lengths Δx and Δz respectively. Applying Snell's law, the correction lengths are obtained as $\Delta x = (W/2)\tan(\varphi_r)$ and $\Delta z = (W/2)\tan(\theta_r)$. The distance of the jet axis plane from the front glass panel is $W/2$, and φ_r and θ_r are angles computed as

$$\phi_r = \sin^{-1}\left(\sin\phi_i \frac{n_a}{n_w}\right) \quad \text{and} \quad \theta_r = \sin^{-1}\left(\sin\theta_i \frac{n_a}{n_w}\right), \tag{A 1}$$

where

$$\phi_i = \tan^{-1}\left(\frac{x_g}{Y}\right) \quad \text{and} \quad \theta_i = \tan^{-1}\left(\frac{z_g}{Y}\right), \tag{A 2}$$

and n_a, n_w are the refractive indices of air and water respectively. The glass panel thickness has been neglected in these calculations. The magnitude of the corrections ($\Delta x/x$ and $\Delta z/z$) made did not exceed 7%. The error in the computation of the actual coordinates of the jet trajectory is of the order of 2.5 mm, the length that corresponds to the pixel size.

Appendix B. Initial conditions of experimental data

Q (cm^3 s^{-1})	$\Delta\rho/\rho_o$ (%)	N^{-2} (s^{-2})	R_o	Re	Q (cm^3 s^{-1})	$\Delta\rho/\rho_o$ (%)	N^{-2} (s^{-2})	R_o	Re
46.76	1.09	0.130	0.052	5180	29.72	0.05	0.116	0.017	3290
38.32	1.09	0.130	0.063	4240	43.40	0.05	0.116	0.012	4810
9.32	1.09	0.130	0.260	1030	10.52	0.02	0.140	0.031	1170
46.76	0.95	0.100	0.048	5180	15.02	0.02	0.140	0.022	1660
39.73	0.95	0.100	0.057	4400	25.35	0.02	0.140	0.013	2810
25.65	0.95	0.100	0.088	2840	35.75	0.02	0.140	0.009	3960
22.42	0.95	0.100	0.101	2480	43.96	0.02	0.140	0.007	4870
10.83	0.95	0.100	0.209	1200	11.43	0.07	0.106	0.053	1270
7.50	0.95	0.100	0.302	830	16.51	0.07	0.106	0.037	1830
12.03	1.05	0.103	0.198	1330	29.72	0.07	0.106	0.021	3290
29.72	1.05	0.103	0.080	3290	32.60	0.07	0.106	0.019	3610
41.15	1.05	0.103	0.058	4560	39.17	0.07	0.106	0.016	4340
46.76	1.05	0.103	0.051	5180	45.92	0.07	0.106	0.013	5080
10.22	0.97	0.077	0.223	1130	12.03	0.109	0.101	0.064	1330
25.06	0.97	0.077	0.091	2780	16.21	0.109	0.101	0.047	1800
39.45	0.97	0.077	0.058	4370	29.14	0.109	0.101	0.026	3230
45.08	0.97	0.077	0.050	4990	36.61	0.109	0.101	0.021	4050
15.02	0.05	0.146	0.034	1660	42.28	0.109	0.101	0.018	4680
28.27	0.05	0.146	0.018	3130	9.92	0.0099	0.077	0.023	1100
38.32	0.05	0.146	0.013	4240	15.92	0.0099	0.077	0.014	1760
45.08	0.05	0.146	0.011	4990	23.89	0.0099	0.077	0.010	2650
12.03	0.13	0.108	0.069	1330	35.18	0.0099	0.077	0.007	3900
19.48	0.13	0.108	0.043	2160	43.40	0.0099	0.077	0.005	4810
36.32	0.13	0.108	0.023	4020	12.03	0.467	0.066	0.132	1330
41.15	0.13	0.108	0.020	4560	18.89	0.467	0.066	0.084	2090
46.76	0.13	0.108	0.018	5180	32.60	0.467	0.066	0.049	3610
10.83	0.15	0.103	0.083	1200	41.71	0.467	0.066	0.038	4620
20.95	0.15	0.103	0.043	2320	46.76	0.467	0.066	0.034	5180
28.85	0.15	0.103	0.031	3190	10.22	2.442	0.043	0.354	1130
38.32	0.15	0.103	0.023	4240	25.65	2.442	0.043	0.141	2840
43.12	0.15	0.103	0.021	4770	40.58	2.442	0.043	0.089	4490
11.13	0.05	0.116	0.046	1230	18.00	2.442	0.043	0.201	1990
13.53	0.05	0.116	0.038	1500	9.02	2.442	0.043	0.401	1000
20.66	0.05	0.116	0.025	2290					

TABLE 2. Initial conditions of experiments of round ($d = 1$ cm) vertical jets in a linearly density-stratified ambient by Konstantinidou & Papanicolaou (2003).

d (cm)	Q (cm^3 s^{-1})	$\Delta\rho/\rho_o$ (%)	R_o	Re
0.50	26.39	1.09	0.016	5840
0.50	22.82	1.09	0.019	5050
0.50	26.39	1.58	0.02	5840
0.50	16.15	0.70	0.021	3980
0.50	22.82	1.58	0.023	5050
0.50	21.03	1.58	0.025	4660
0.50	15.67	1.58	0.033	3470
0.75	26.32	0.70	0.035	4320
0.50	12.10	1.58	0.043	2680
0.50	9.07	1.68	0.058	2010
0.50	9.95	2.45	0.065	2200
0.50	7.66	1.58	0.069	1700
0.50	9.07	2.45	0.071	2010
0.50	8.19	2.45	0.079	1810
0.50	7.30	2.35	0.088	1620
0.50	7.30	2.45	0.089	1620
1.00	38.04	2.35	0.095	4210

TABLE 3. Initial conditions of experiments of round vertical negatively buoyant jets in a homogeneous ambient by Papanicolaou & Kokkalis (2008).

Θ (deg.)	d (cm)	Q (cm^3 s^{-1})	$\Delta\rho/\rho_a$	R_o	Re_o
45	0.6	31.51	2.07	0.030	6690
45	0.6	40.94	2.06	0.023	8690
45	0.6	51.50	2.06	0.018	10930
45	0.6	60.51	2.03	0.015	12840
45	0.6	33.02	3.05	0.034	7010
45	0.6	45.64	3.04	0.025	9680
45	0.6	54.72	3.04	0.021	11610
45	0.6	29.64	3.05	0.038	6290
60	0.6	37.63	2.49	0.027	7990
60	0.6	49.74	2.47	0.020	10550
60	0.6	57.62	2.43	0.017	12230
60	0.6	39.53	3.52	0.031	8390
60	0.6	52.75	3.49	0.023	11200
60	0.6	31.25	3.01	0.036	6630
60	0.6	43.26	3.00	0.026	9180
60	0.6	50.95	2.07	0.018	10810
75	0.6	29.37	3.11	0.039	6230
75	0.6	33.87	3.12	0.034	7190
75	0.6	37.95	3.14	0.030	8050
75	0.6	43.26	3.13	0.026	9180
75	0.6	54.57	3.12	0.021	11580
75	0.6	57.19	3.12	0.020	12140
75	0.6	49.57	3.12	0.023	10520

TABLE 4. Initial conditions of experiments of inclined negatively buoyant jets in homogeneous ambient by Papakonstantis *et al.* (2007).

REFERENCES

ABRAHAM, G. 1967 Jets with negative buoyancy in homogeneous fluid. *J. Hydraul. Res.* **5**, 235–248.

BAINES, W. D., TURNER, J. S. & CAMPBELL, I. H. 1990 Turbulent fountains in an open chamber. *J. Fluid Mech.* **212**, 557–592.

Bloomfield, L. J. & Kerr, R. C. 1998 Turbulent fountains in a stratified fluid. *J. Fluid Mech.* **358**, 335–356.

Bloomfield, L. J. & Kerr, R. C. 2000 A theoretical model of a turbulent fountain. *J. Fluid Mech.* **424**, 197–216.

Bloomfield, L. J. & Kerr, R. C. 2002 Inclined turbulent fountains. *J. Fluid Mech.* **451**, 283–294.

Carazzo, G., Kaminski, E. & Tait, S. 2006 The route to self-similarity in turbulent jets and plumes. *J. Fluid Mech.* **547**, 137–148.

Fan, L. N. 1967 Turbulent buoyant jets into stratified or flowing ambient fluids. Tech. Rep. KH-R-15, W. M. Keck Laboratory of Hydraulics and Water Resources, California Institute of Technology, Pasadena, CA, USA.

Fischer, H. B., List, E. J., Koh, R. C. Y., Imberger, J. & Brooks, N. H. 1979 *Mixing in Inland and Coastal Waters.* Academic.

Hutter, K. & Hofer, K. 1978 Freistrahlen im homogenen und stratifizierten Medium—ihre Theorie und deren Vergleich mit dem Experiment. *Mitteilungen der Versuchsanstalt für Wasserbau, Hydrologie und Glaziologie*, ETH Zürich, Nr. 27.

Jirka, G. H. 2004 Integral model for turbulent buoyant jets in unbounded stratified flows: part I; single round jet. *Env. Fluid Mech.* **4**, 1–56.

Kaminski, E., Tait, S. & Carazzo, G. 2005 Turbulent entrainment in jets with arbitrary buoyancy. *J. Fluid Mech.* **526**, 361–376.

Konstantinidou, K. & Papanicolaou, P. N. 2003 Vertical round and orthogonal buoyant jets in a linear density-stratified fluid. In *Proc. 30th IAHR Congress on Water Engineering and Research in a Learning Society: Modern Developments and Traditional Concepts; Inland Waters—Research, Engineering and Management Theme* (ed. J. Ganoulis & P. Prinos; theme ed. I. Nezu & N. Kotsovinos), vol. 1, pp. 293–300.

Lindberg, W. R. 1994 Experiments on negatively buoyant jets, with or without cross-flow. In *Recent Research Advances in the Fluid Mechanics of Turbulent Jets and Plumes* (ed. P. A. Davies & M. J. Valente Neves), pp. 131–145. Kluwer.

List, E. J. 1982 Mechanics of turbulent buoyant jets and plumes. In *Turbulent Buoyant Jets and Plumes* (ed. W. Rodi), pp. 1–68. Pergamon.

List, E. J. & Imberger, J. 1973 Turbulent entrainment in buoyant jets and plumes. *J. Hydraul. Div. ASCE* **99**, 1461–1474.

Papakonstantis, I., Kampourelli, M. & Christodoulou, G. 2007 Height of rise of inclined and vertical negatively buoyant jets. In *Proc. 32nd IAHR Congress: Harmonizing the Demands of Art and Nature in Hydraulics; Fluid Mechanics and Hydraulics Theme* (ed. G. Di Silvio & S. Lanzoni; theme ed. A. Cenedese), CD-ROM.

Papanicolaou, P. N. & Kokkalis, T. J. 2008 Vertical buoyancy preserving and non-preserving fountains, in a homogeneous calm ambient. *Intl J. Heat Mass Transfer* **51**, 4109–4120.

Papanicolaou, P. N. & List, E. J. 1988 Investigations of round vertical turbulent buoyant jets. *J. Fluid Mech.* **195**, 341–391.

Priestley, C. H. B. & Ball, F. K. 1955 Continuous convection from an isolated source of heat. *Q. J. R. Met. Soc.* **81**, 144–157.

Roberts, P. J. W., Ferrier, A. & Daviero, G. 1997 Mixing in inclined dense jets. *ASCE J. Hydraul. Engng* **123**, 693–699.

Roberts, P. J. W. & Toms, G. 1987 Inclined dense jets in flowing current. *ASCE J. Hydraul. Engng ASCE* **113**, 323–341.

Rouse, H., Yih, C. S. & Humphreys, H. W. 1952 Gravitational convection from a boundary source. *Tellus* **4**, 201–210.

Turner, J. S. 1966 Jets and plumes with negative or reversing buoyancy. *J. Fluid Mech.* **26**, 779–792.

Turner, J. S. 1986 Turbulent entrainment: the development of the entrainment assumption, and its application to geophysical flows. *J. Fluid Mech.* **173**, 431–471.

Wang, H. & Law, A. W.-K. 2002 Second-order integral model for a round turbulent buoyant jet. *J. Fluid Mech.* **459**, 397–428.

Wong, D. R. & Wright, S. J. 1988 Submerged turbulent buoyant jets in stagnant linearly stratified fluids. *J. Hydraul. Res.* **26**, 199–223.

Woods, A. W. & Caulfield, C. P. 1992 A laboratory study of explosive volcanic eruptions. *J. Geophys. Res.* **97**, 6699–6712.

Yannopoulos, P. C. 2006 An improved integral model for plane and round turbulent buoyant jets. *J. Fluid Mech.* **547**, 267–296.

Zeitoun, M. A., McIlhenny, W. F. & Reid, R. O. 1970 Conceptual designs of outfall systems for desalting plants. *R & D Progress Report No. 550*, Office of Saline Water, US Dept. of Interior, Washington, DC, USA, p. 139.

Zhang, H. & Baddour, R. E. 1998 Maximum penetration of vertical round dense jets at small and large Froude numbers. *ASCE J. Hydraul. Engng.* **124**, 550–553.